Natural convection in Bingham plastic fluids from two heated horizontal cylinders in a square duct

Lubhani Mishra and Raj P. Chhabra

Department of Chemical Engineering, IIT Kanpur, India 208016

ABSTRACT

Laminar natural convection has been numerically investigated from two cylinders in a square duct filled with a Bingham plastic fluid. The effect of Rayleigh, Prandtl and Bingham numbers has been elucidated by solving the coupled governing differential equations over the following ranges of conditions: $10^4 \leq Ra \leq 10^6$; $10 \leq Pr \leq 100$ and $0.01 \leq Bn \leq Bn_{max}$.

INTRODUCTION

Most structured fluids like suspensions, emulsions, micellar solutions, and high molecular weight composites exhibit a yield stress[1,2]. These so-called visco-plastic substances display both solid-like and fluid-like rheological behavior depending upon the magnitude of the external applied stress vis-a-vis the fluid yield stress. This dual nature poses difficulty in predicting the flow and heat transfer characteristics of these materials.

Over the years, many investigators have focused on the buoyancy-induced convection from circular cylinders located concentrically or eccentrically within square or rectangular ducts. In recent years, some work has also been carried out with a pair of heated circular cylinders placed inside a square duct, e.g., see Yoon et al.[3,4] for Newtonian fluids. Effect of confinement on free convection in Bingham plastic fluids has also been explored. For instance, Turan et al.[5] have investigated laminar natural convection in a square duct while Sairamu et al.[6] studied convection from a circular cylinder confined in a duct. It is worthwhile to add here that the available literature on free convection in Bingham plastic fluids is rather limited. Baranwal and Chhabra[7] examined the effect of yield-stress on a pair of horizontally aligned cylinders in a square duct and this work aims to investigate the complex interplay of the aforementioned parameters in a similar fashion for two vertically aligned cylinders in a square duct. The present study endeavors to develop insights into the momentum and heat transfer characteristics in a confined geometry of two identical, vertically aligned cylinders in a square duct filled with a Bingham plastic fluid. Also, the effect of the pertinent dimensionless groups, namely, Rayleigh number (Ra), Prandtl number (Pr) and Bingham number (Bn) over the following ranges of conditions: $10^4 \leq Ra \leq 10^6$; $10 \leq Pr \leq 100$ and $0.01 \leq Bn \leq Bn_{max}$ is also elucidated.

PROBLEM FORMULATION

In the present study, two vertically-aligned infinitely long horizontal cylinders, each of radius R, are placed coaxially in an infinitely long square duct of side L such that the centers of the two cylinders lie on the vertical center-line of the duct and are equidistant from the center of the duct (Fig. 1). The z-dimension is considered to be infinite so that the flow can be approximated as two-dimensional. The radius-to-side length ratio is held fixed as $R/L = 0.2$ and the two cylinders are separated by the fixed distance of $0.5L$. The intervening space is filled with an incompressible Bingham plastic fluid. Both cylinders are heated to maintain their surfaces at temperature, T_H, whereas, isothermal boundary conditions are imposed at the duct walls at low temperature, T_C which is also used as the reference temperature for the fluid medium. The thermo-physical properties of the fluid are assumed to be independent of the temperature and calculated at the mean film temperature, $T_f = (T_H+T_C)/2$ except for the fluid density in the buoyancy term which follows the Boussinesq approximation as:

$$\rho_C - \rho = \rho_C \beta (T - T_C) \tag{1}$$

The coupled governing equations in their dimensionless forms are written below:

Equation of continuity:

$$\nabla \bullet \boldsymbol{V} = 0 \tag{2}$$

Momentum equation:

$$(\boldsymbol{V} \bullet \nabla)\boldsymbol{V} = -\nabla P + \sqrt{\frac{Pr}{Ra}}(\nabla \bullet \boldsymbol{\tau}) + \Theta \boldsymbol{e}_y \tag{3}$$

Thermal energy equation:

$$(\boldsymbol{V} \bullet \nabla)\Theta = \frac{1}{\sqrt{Ra\,Pr}}(\nabla^2 \Theta) \tag{4}$$

The Bingham plastic constitutive equation[8] is given as:

$$\boldsymbol{\tau} = \left(1 + \frac{Bn}{|\dot{\gamma}|}\right)\dot{\gamma} \quad \text{if } |\boldsymbol{\tau}| \geq Bn \tag{5}$$

$$\dot{\gamma} = 0 \quad \text{if } |\boldsymbol{\tau}| < Bn \tag{6}$$

The variables appearing in the above equations are rendered dimensionless using $2R$ and U_C as the scaling variables for length and velocity, respectively. Thus, the dimensionless groups appearing in Eqs. 2-4 can be defined as below (where symbols are defined in the nomenclature):

$$Ra = \frac{\rho_C{}^2 C_P g \beta (T_H - T_C)(2R)^3}{\mu_B k}; \quad Pr = \frac{C_P \mu_B}{k}$$

and $Bn = \dfrac{\tau_o (2R)}{\mu_B U_C}$.

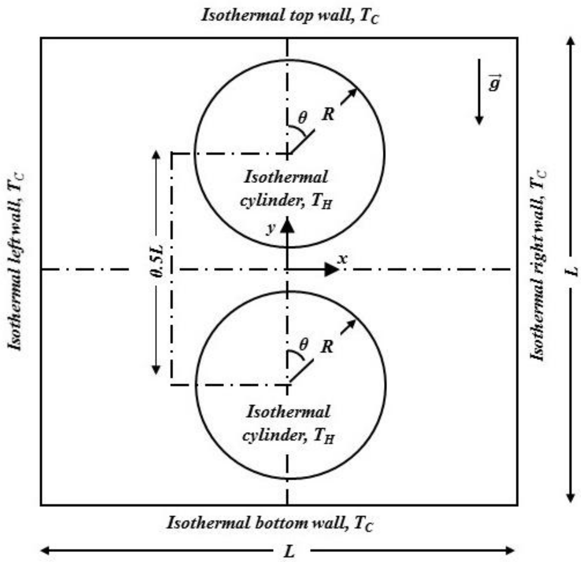

Figure 1. Schematic of the flow configuration.

The inherent discontinuity in the constitutive equations for yield-stress fluids, Eqs. 5 and 6, has been treated by employing the Papanastasiou regularization[9] which enables the Bingham plastic viscosity to be approximated as:

$$\boldsymbol{\tau} = \left(1 + \frac{[1 - \exp(-M|\dot{\gamma}|)]Bn}{|\dot{\gamma}|}\right)\dot{\gamma} \tag{7}$$

NUMERICAL SOLUTION SCHEME

The coupled governing equations, Eqs. 2-4, have been solved along with the prescribed boundary conditions (no-slip for velocity and isothermal temperature conditions on the cylinder and duct walls) using a finite element based method, COMSOL Multiphysics (Version 4.3a). The symmetry along the vertical center-line is exploited and simulations are performed only for half domain which is discretized using quadrilateral elements forming a mesh structure. In the vicinity of the cylinders, the mesh is made coarser by a gradual increment in the element size by using a smoothing function which leads to a smooth transition from fine to coarse grids to capture the steep gradients near the surface of cylinders. A steady, 2-D and laminar module was used in conjunction with the heat transfer module for fluids which was solved using a linear direct solver (PARDISO). A relative tolerance of 10^{-5} is used as the convergence criterion for the momentum and energy equations. Also, the yield surfaces were delineated by using the von Mises yielding criterion[7] with a relative tolerance level of 10^{-6}.

Table 1. Effect of grid on average Nusselt number and drag coefficient.

Grid independence test ($Ra = 10^6$, $Pr = 100$)				
Grid (elements)	$Bn = 0.01$			
	Nu_{upper}	Nu_{lower}	C_{Dupper}	C_{Dlower}
G1 (9957)	3.2766	6.1272	-0.1358	-0.0365
G2 (18618)	3.2937	6.1623	-0.1359	-0.0365
G3 (34414)	3.3039	6.1817	-0.1360	-0.0366
Grid (elements)	$Bn = 10$			
	Nu_{upper}	Nu_{lower}	C_{Dupper}	C_{Dlower}
G1 (9957)	2.8313	2.8314	-0.0549	-0.0549
G2 (18618)	2.8461	2.8461	-0.0549	-0.0549
G3 (34414)	2.8547	2.8547	-0.0549	-0.0549

In order to ensure that the solution is free from the grid effects, grid independence tests were carried out with different grids, namely, G1, G2 and G3, varying from coarse to fine (Table 1). These tests were performed at the maximum values of the Rayleigh and Prandtl numbers used in this study. The results are tabulated at extreme values of the Bingham number to confirm the adequacy of the chosen grid for resolving the yielded as well as unyielded regions. The values of the average Nusselt number and drag coefficient for both cylinders changed by less than 1% between grids G2 and G3. Hence, the grid G2 was regarded to be sufficient to resolve the velocity and temperature fields.

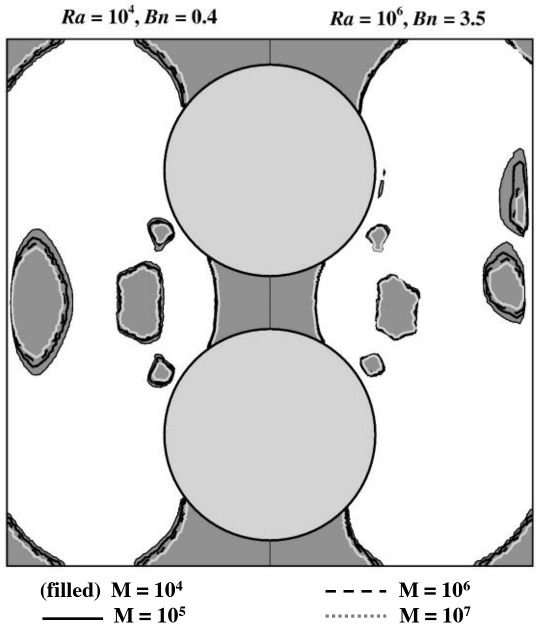

Figure 2. Effect of Papanastasiou regularization parameter on yielded (unshaded)/unyielded (shaded) regions.

In order to approximate the fluid behavior as close to the true Bingham fluid as possible, as large a value of the regularization parameter, M must be chosen in Eq. 7 as possible. The effect of M on the yielded/unyielded regions in the domain is shown in Fig. 2 where $M = 10^6$ has been found to be satisfactory. Similarly, the resulting values of the Nusselt number and drag coefficient had also stabilized up to five significant digits at $M = 10^6$.

RESULTS AND DISCUSSION

The results are presented and discussed for the momentum and heat transfer characteristics and, in particular, consideration is given to the delineation of the yielded/unyielded surfaces, streamlines, isotherm contours, and local and average Nusselt numbers as the functions of the aforementioned governing parameters.

Validation of results

In order to check the reliability and precision of our solution procedure, benchmark comparisons were made with that of Yoon et al.[3] for air. A good correspondence (within 1%) is seen in Table 2 for the values of the average Nusselt number for both cylinders. Similarly, the present predictions of the non-dimensionalized temperature and velocity profiles are in excellent agreement with that of Turan et al.[5] in a two-dimensional square duct (within ± 0.5%).

Table 2. Comparison of the present average Nusselt numbers with that of Yoon et al.[3].

	Present	Yoon et al.[3]
	$Ra = 10^4$	
Upper cylinder	3.0433	3.0462
Lower cylinder	11.1791	11.1603
	$Ra = 10^5$	
Upper cylinder	4.3747	4.3220
Lower cylinder	12.9628	13.0802

Structure of yield surfaces

Representative results on the structure and location of the yield surfaces are shown in Fig. 3 which demarcate the fluid-like (yielded) and solid-like (unyielded) regions in the flow domain based on the prevailing stress levels. At low values of the Bingham number, the entire fluid is yielded (analogous to a Newtonian fluid). At fixed Rayleigh and Prandtl numbers, these regions progressively shrink with the increasing Bingham number until the limiting value is reached (Bn_{max}) where the entire fluid becomes unyielded and conduction is the dominant mode of heat transfer. Such values of the Bn_{max} are summarized in Table 3 for each combination of the Rayleigh and Prandtl numbers beyond which there is no effect of Bingham number on yield surfaces or Nusselt number. As expected, Bn_{max} bears a positive dependence on the Rayleigh number.

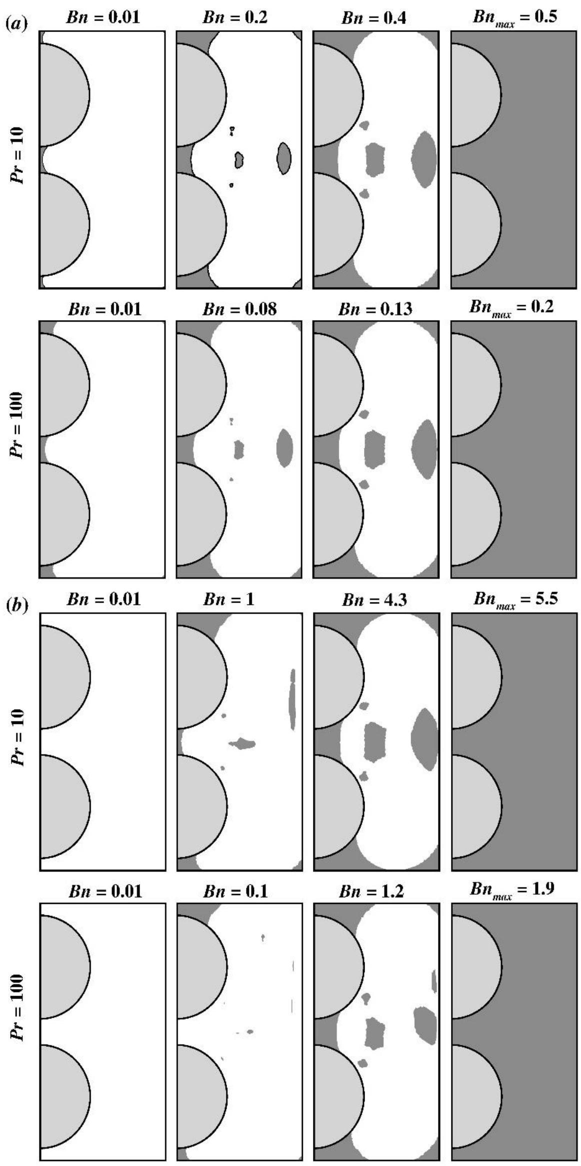

Figure 3. Representative yielded (unshaded)/unyielded regions (shaded) at (*a*) $Ra = 10^4$ and (*b*) $Ra = 10^6$.

Table 3. Maximum Bingham number, Bn_{max} as a function of Rayleigh number (Ra) and Prandtl number (Pr).

Ra	Pr			
	10	30	50	100
10^4	0.5	0.4	0.3	0.2
10^5	1.8	1.1	0.8	0.6
10^6	5.5	3.4	2.5	1.9

Streamlines and isotherm contours

Representative streamlines (right half) and isotherm contours (left half) are shown in Fig. 4 for scores of values of the Bingham number and two extreme values of the Prandtl number at the maximum value of Ra = 10^6. The corresponding patterns at Ra = 10^3 and 10^4 are not shown here for conciseness but are qualitatively similar to that seen in Fig. 4. The fluid in the vicinity of the heated cylinders gets heated and rises upwards and comes in contact with the cold duct walls leading to single-celled recirculatory zones. An increase in the uniformity of these vortices is observed with an increase in the Bingham number due to the balance of high convective currents at high Rayleigh number by the increased value of the fluid yield stress. Similarly, the distorted isotherm contours at low Bingham number are marked by the upward rising thermal plume near the heated cylinders which is restricted by the cold fluid as well as cold duct walls. With the formation of unyielded regions in the domain at high Bingham numbers, the isotherm contours follow the body contours (concentric circles) thereby highlighting the dominance of conduction at high Bingham numbers.

At low Rayleigh numbers, the limiting value of the Bingham number, Bn_{max}, is low as shown in Table 3 due to the low convective velocity which is easily countered with the increasing fluid yield stress. Thus, the distortion of streamlines and thermal plume are both suppressed and these follow regular concentric patterns even at low Bingham numbers. The effect of increasing the Prandtl number at a fixed Rayleigh number is observed in terms of reduction in the spread of the heated fluid in the domain owing to the lowering of the Grashof numbers, i.e., low convective velocity and this effect is more pronounced at low Bingham numbers.

Thus, in summary, it can be said that the flow and heat transfer in the confined

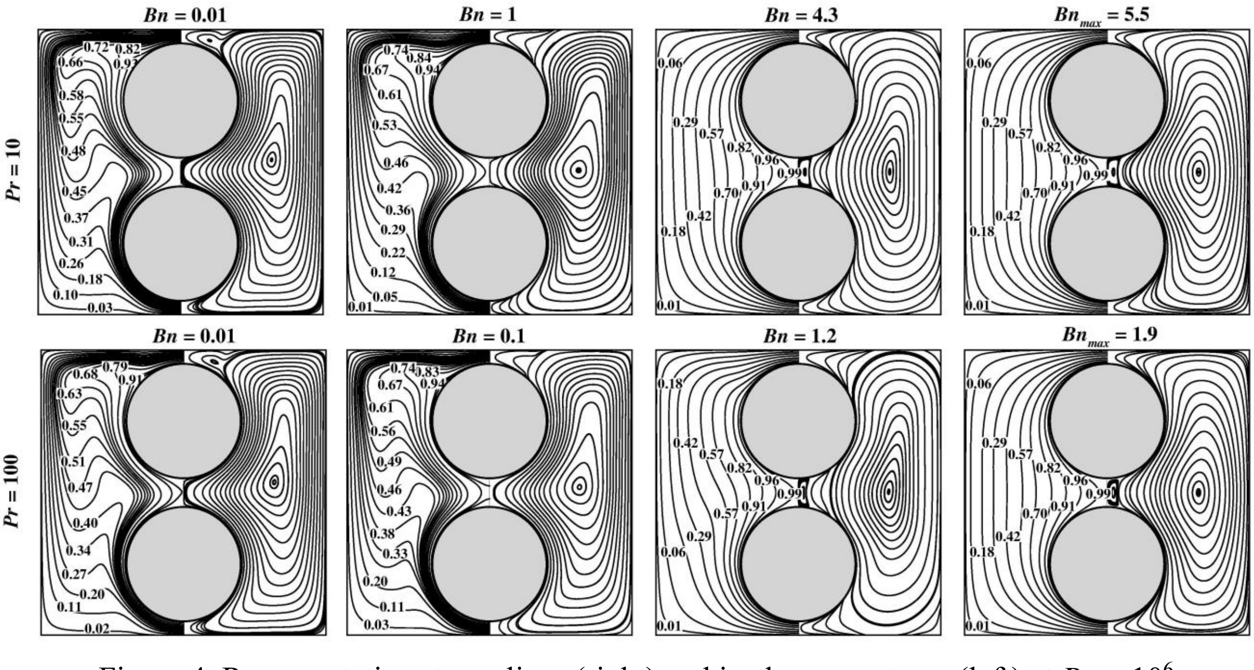

Figure 4. Representative streamlines (right) and isotherm contours (left) at $Ra = 10^6$.

domain is a result of a complex interplay of the convective transport of fluid and the fluid yield stress and larger fluid circulation and dispersion of heated fluid is observed at low values of the Prandtl and Bingham numbers but at high values of Rayleigh number.

Local Nusselt number

Typical local Nusselt number distribution is shown in Fig. 5 on the surfaces of the upper (Nu_{upper}) and lower (Nu_{lower}) cylinders for a range of values of the Bingham number at the extreme values of the Prandtl and Rayleigh numbers, i.e., Pr = 10 and 100 at Ra = 10^4 and 10^6. The curves for the upper and lower cylinders follow an opposite trend where maxima in both the cases is observed when the cylinder surface is closest to the wall (θ = 180° for the upper cylinder and θ = 0° for the lower cylinder). This is due to the presence of steep temperature gradients between the surfaces of the heated cylinders and the cold duct walls. The rate of heat transfer varies monotonically as we move further along the surface of both cylinders. The minimum heat transfer occurs at θ = 0° and θ = 180° for the upper and lower cylinders, respectively where the surfaces of the two cylinders are the closest, resulting in the lowest temperature gradients. The curvature effects of the cylinders cause a slight variation in the slope of the curves near the mid-point on the cylinder surface.

The effect of the Prandtl number is seen to be rather weak when its value is increased from Pr = 10 to Pr = 100 except a slight decrease in the rate of heat transfer due to the concomitant decrease in Grashof number. For the upper cylinder, the peaks and troughs, thus formed, between θ = 30° to θ = 150° are due to the dispersion of thermal plume near the upper part of the cylinder. On the other hand, the variation in these curves is still monotonic for the lower cylinder with an increased rate of heat transfer due to high velocity of the heated fluid in the vicinity of the cylinder. Lastly, the overlapping plots at all values of Bingham number for Ra = 10^4 indicate the dominance of conduction at low Rayleigh numbers. Similar behavior is also obtained at high Bingham numbers at Ra = 10^6 where the fluid becomes unyielded everywhere. Overall, the high rates of heat transfer are obtained at low Bingham numbers and high Rayleigh numbers where most of the fluid is yielded which promote convective heat transfer.

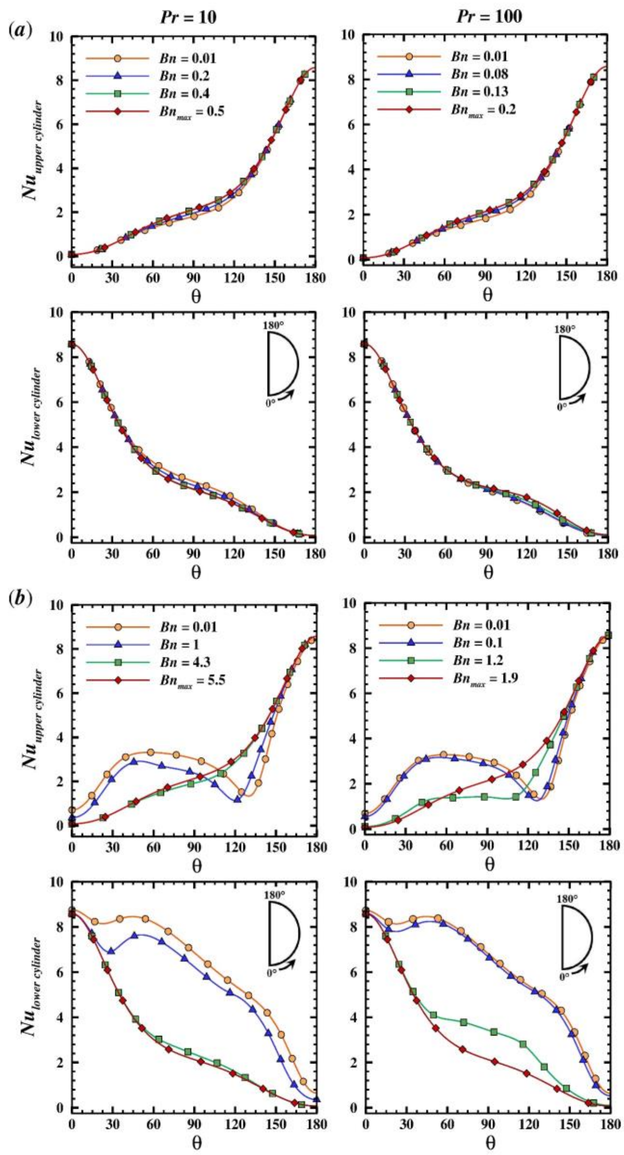

Figure 5. Local Nusselt number distribution at (a) Ra = 10^4 and (b) Ra = 10^6.

Average Nusselt number

The averaging of the local Nusselt number values shown in Fig. 5 over the cylinder surface leads to the average Nusselt number as shown in Fig. 6 for the range of Rayleigh, Prandtl and Bingham numbers spanned in this study for the upper and lower cylinders separately. An opposite behaviour is observed for the upper and lower cylinders in correspondence with the local plots of Nusselt number (Fig. 5). Moreover, at low Rayleigh numbers, i.e., $Ra = 10^4$ and even $Ra = 10^5$, the variation in the value of average Nusselt number with Bingham number for all values of Prandtl number is very small, highlighting the dominance of conduction in this range of parameters as postulated earlier. As the Rayleigh number is increased, buoyancy-induced flow strengthens and heat transfer is seen to fall below the conduction limit at low Bingham numbers for the upper cylinder. This is due to the reduction in driving force for heat transfer from the upper cylinder owing to the pre-heating of the fluid by the lower cylinder. Overall, for sufficiently large values of the Bingham number, the average Nusselt number reaches its asymptotic value commensurate with its conduction limit. It should be noted that larger values of Rayleigh number require higher values of the Bingham number to approach this limit. Thus, it can be concluded that the value of the average Nusselt number is a result of an intricate interplay between the Bingham, Rayleigh and Prandtl numbers as well as the geometric factors.

CONCLUSIONS

In this work, the steady laminar natural convection heat transfer in Bingham plastic fluids from two heated cylinders confined in a cold square duct has been studied numerically over the ranges of conditions: $10^4 \leq Ra \leq 10^6$, $10 \leq Pr \leq 100$ and $0.01 \leq Bn \leq Bn_{max}$. The numerical data obtained for velocity and thermal fields is interpreted in terms of the structure of the yield surfaces, streamlines and isotherm contours, maximum Bingham number, and local and average Nusselt number. At fixed Rayleigh and Prandtl numbers, the increase in the Bingham number leads to the formation of unyielded regions in the fluid domain and the entire fluid effectively becomes unyielded as the limiting Bingham number is approached. These unyielded (solid-like) regions are dominated by conduction as the primary mode of heat transfer while convective heat transfer exists in the yielded (fluid-like) regions. The flow patterns and rate of heat transfer is highly influenced by the presence of such yielded/unyielded zones in the confined fluid domain. It can be concluded that the Nusselt number shows an inverse dependence on the Bingham and Prandtl numbers while it shows a positive dependence on the Rayleigh number for a given geometrical configuration.

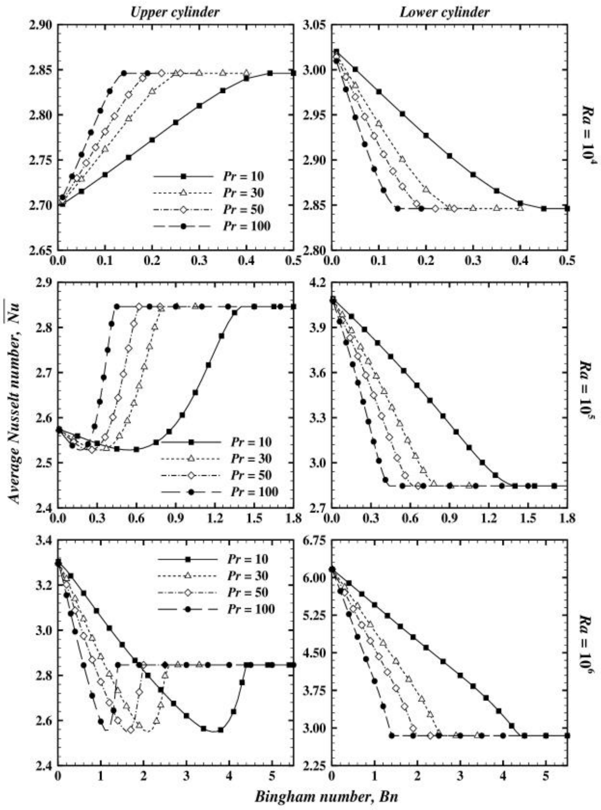

Figure 6. Dependence of the average Nusselt number on Bingham, Rayleigh and Prandtl numbers for the upper (left column) and lower (right column) cylinders.

ACKNOWLEDGMENT

RPC would like to gratefully acknowledge the award of the JC Bose Fellowship to him (SB/S2/JCB-06/2014) by the Department of Science & Technology, New Delhi, India for the period 2015-2020.

NOMENCLATURE

C_D: Drag coefficient $\left(=\dfrac{F_D}{\rho_C U_C{}^2 R}\right)$, (-)

C_P: Heat capacity of fluid, $J.kg^{-1}.K^{-1}$

$\boldsymbol{e}_y$: Unit vector in y-direction, (-)
g: Acceleration due to gravity, $m.s^{-2}$
h: Local heat transfer coefficient, $W.m^{-2}.K^{-1}$
k: Thermal conductivity of fluid, $W.m^{-1}.K^{-1}$
M: Growth rate parameter, (-)

Nu: Local Nusselt number $\left(=\dfrac{h(2R)}{k}\right)$, (-)

$\overline{Nu}$: Average Nusselt number, (-)
P: Dimensionless pressure, (-)
T_C: Cold fluid and duct temperature, K
T_H: Hot cylinder temperature, K
U_C: Reference velocity $\left(=\sqrt{2Rg\beta\Delta T}\right)$, $m.s^{-1}$
$\boldsymbol{V}$: Dimensionless velocity vector, (-)

Greek symbols
β: Coefficient of volume expansion, K^{-1}
∇: Del operator, m^{-1}
$\dot{\gamma}$: Rate of strain tensor, (-)
μ_B: Bingham plastic viscosity, $Pa.s$
ρ: Density of the fluid, $kg.m^{-3}$
ρ_C: Density of the fluid at T_C, $kg.m^{-3}$
θ: Position on the surface of cylinder, degree

Θ: Dimensionless temperature $\left(=\dfrac{T - T_C}{T_H - T_C}\right)$, (-)

τ: Extra stress tensor, (-)
τ_o: Yield stress, Pa

REFERENCES

1. Chhabra, R.P., and Richardson, J.F. (2008), "Non-Newtonian Flow and Applied Rheology, Second edition", Butterworth-Heinemann: Oxford, UK.

2. Barnes, H.A. (1999), "The Yield Stress- a Review or 'παντα ρει'- Everything Flows?", *J. Non-Newt. Fluid Mech.*, **81**, 133-178.

3. Yoon, H.S., Jung, J.H., and Park, Y.G., (2012), "Natural Convection in a Square Enclosure with Two Horizontal Cylinders", *Numer. Heat Transfer A*, **62**, 701-721.

4. Yoon, H.S., Park, Y.G., and Jung, J.H., (2013), "Natural Convection in a Square Enclosure with Differentially Heated Two Horizontal Cylinders", *Numer. Heat Transfer A*, **65**, 302-326.

5. Turan, O., Chakraborty, N., and Poole, R. J., (2010), "Laminar Natural Convection of Bingham Fluids in a Square Enclosure with Differentially Heated Side Walls", *J. Non-Newt. Fluid Mech.*, **165**, 901–913.

6. Sairamu, M., Nirmalkar, N., and Chhabra, R. P., (2013), "Natural convection from a Circular Cylinder in Confined Bingham Plastic Fluids", *Int. J. Heat Mass Transfer*, **60**, 567–581.

7. Baranwal, A.K., and Chhabra, R.P., (2017), "Effect of fluid yield stress on natural convection from horizontal cylinders in a square enclosure", *Heat Transfer Eng.*, **38**, 557-577.

8. Bird, R.B., Armstrong, R.C., and, Hassager, O., (1987), "Dynamics of Polymeric Liquids, Vol. 1: Fluid Dynamics, Second edition", Wiley, New York.

9. Papanastasiou, T. C., (1987), "Flow of Materials with Yield", *J. Rheol.*, **31**, 385-404.